Environ Earth Sci (2016) 75:1061
DOI 10.1007/s12665-016-5858-0

ORIGINAL ARTICLE

Stable carbon and oxygen isotopes of terra rossa in Guizhou Province of China and their relationship to climate and ecology

Daojing Li[1] · Hongbing Ji[1,2] · Xiao Wei[1] · Shijie Wang[1]

Received: 29 June 2015 / Accepted: 23 June 2016 / Published online: 2 July 2016

Abstract This paper analyzed stable carbon and oxygen isotopic changes in organic matter ($\delta^{13}C_{SOM}$) and disseminated carbonate ($\delta^{13}C_{SC}$ and $\delta^{18}O_{SC}$) in four terra rossa profiles in Gouzhou, southwestern China. The objectives were to understand more information about climate change in this area and to determine whether the isotope values of disseminated carbonate in terra rossa preserved a record of environmental change and to distinguish environmental sources that may have influenced the isotopic chemistry. Results suggested that carbonate in terra rossa is mainly pedogenic carbonate, and its formation is closely associated with root activities. The $\delta^{13}C_{SOM}$ variations indicate a climate change into warmer and drier conditions at about 6000–8000 a BP, 12000–14000 a BP and 28000 a BP. Plants were more depleted in $\delta^{13}C$ when carbonate precipitated. Compared with the $\delta^{13}C_{SOM}$, the $\delta^{13}C_{SC}$ tends to reflect more average climate change information. Most large variations of the $\delta^{13}C_{SC}$ and $\delta^{13}C_{SOM}$ between adjacent sampling layers are accompanied with the change in soil color and texture, suggesting a certain connection between the $\delta^{13}C$ and the soil properties. This study found a positive linearity between $\delta^{13}C_{SC}$ and $\delta^{18}O_{SC}$; a striking different value and correlation coefficient in different sites may provide a meaningful signal of regional climate change.

✉ Hongbing Ji
ji.hongbing@hotmail.com

[1] State Key Laboratory of Environmental Geochemistry, Institute of Geochemistry, Chinese Academy of Sciences, Guiyang 550002, China

[2] College of Civil and Environmental Engineering, University of Science and Technology Beijing, Beijing 100083, China

Keywords Disseminated carbonate · Terra rossa · Stable carbon isotope · Stable oxygen isotope · Soil organic matter

Introduction

The stable carbon and oxygen isotopic composition of soil carbonate ($\delta^{13}C_{SC}$ and $\delta^{18}O_{SC}$) has been used to understand the climatic and ecological changes in many different regions of the world (Stevenson et al. 2005; Schmid et al. 2006; Quade et al. 2007). Soil carbonate includes lithogenic (inherited) and pedogenic (secondary) carbonate. Many of these studies were based on pedogenic carbonate because it is formed in the weathering process and preserves environmental signals and thus can reflect the terrestrial ecosystems and climate change (Cerling 1984; Connin et al. 1997; Pankaj 2001; Stevenson et al. 2005; Kovda et al. 2006; Achyuthan et al. 2007). The lithogenic carbonate and pedogenic carbonate usually coexist in the soil, studying the carbon and oxygen isotopes of pedogenic carbonate, therefore, often needs to separate the pedogenic carbonate from lithogenic carbonate first. Usually, the pedogenic carbonate is studied in the following two conditions: When the carbonate crystal particle is large enough, the pedogenic carbonate is artificially stripped down from the soil structure or the gravel surface it is attached on, or by using microscope, the pedogenic carbonate and lithogenic carbonate are distinguished by their different mineral forms in the soil for further analysis. So the pedogenic carbonate samples in existing research are usually collected from the pedogenic carbonate nodules or the pedogenic carbonate coatings on lithic detritus (Miller et al. 2007; Quade et al. 2007; Kraimer and Monger 2009). Many soils lack carbonate of such form, and it is difficult to

separate the pedogenic carbonate from lithogenic carbonate completely in many cases; the isotopic analysis of carbonate is therefore necessarily restricted to disseminated carbonate which is the mixture of carbonate in all forms. However, the research about the isotopic study of disseminated carbonate is less reported.

Macroscopic carbonates usually form under arid climatic conditions (Cerling 1984; Miller et al. 2007; Quade et al. 2007). In Guizhou Province of China, isotopic study about soil carbonate has barely been carried out because macroscopic carbonates are hardly found due to the high precipitation. The climatic or vegetational information contained in the soil carbonate is poorly understood in this area. However, it does not mean the carbonate does not exist. It is found that in Europe, where there is frequently consistent precipitation throughout the year, carbonate leaching is prevalent and soil carbonate can accumulate in regions where carbonate rich bedrocks occur (Candy 2009; Candy et al. 2012). Guizhou Province has widely distributed carbonate rocks, with the carbonate deposition reaching a total thickness of approximately 8500 m, and a wide distribution of terra rossa covers the carbonate bedrock (Liu et al. 2013). It is likely that disseminated carbonate can be found in the terra rossa. According to the field observations, though the macroscopic carbonates were basically not found in soil profiles, the microstructures of carbonate were observed by electron scanning microscope (SEM); carbonate content has also been measured in this study as well as in other studies about terra rossa (Valter et al. 1992; Irmak and Aydemir 2008). Therefore, the isotopic analysis of carbonate in terra rossa is restricted to the disseminated carbonate. Interpretation of it would be difficult because it may reflect a different pedogenic process or inclusion of detrital material.

The stable carbon isotopic composition of soil organic matter ($\delta^{13}C_{SOM}$) has also been used to study vegetation and climate change (Boutton et al. 1998; Landi et al. 2003; Rao et al. 2013), because it reflects the relative contribution of organic matter from C_3 and C_4 plants (Kelly et al. 1991). The carbon isotope composition of pedogenic carbonate is controlled by organic matter over the time of the carbonate formation. Based on the $\delta^{13}C$ model of pedogenic carbonate (Cerling 1984; Quade et al. 1989), at depths below the influence of the atmosphere, an approximately 15 ‰ $\delta^{13}C$ offset exists between the soil organic matter and the pedogenic carbonate. Theoretically, the $\delta^{13}C$ value of pedogenic carbonate can be estimated by measuring the $\delta^{13}C$ value of soil organic matter, if the plants at the time when the pedogenic carbonate was formed were not affected by anthropogenic or natural climate change (Quade et al. 1989, 2007). Therefore, isotopic chemistry of carbonate can be estimated by comparing $\delta^{13}C$ values of the coexisting organic matter pools.

In this study, isotopic information of disseminated carbonate and organic matter in four terra rossa profiles in Guizhou Province, China was explored. The objectives are to understand more information about climate change in this area and to determine whether isotopic values of disseminated carbonate in terra rossa preserve a record of environmental change and to distinguish environmental sources that may have influenced the isotopic chemistry of disseminated carbonate.

Materials and methods

Geological setting

Guizhou Province is located in the west of the Yangtze Platform (Liu et al. 2013). The climate of Guizhou Province occurs in the transition zone between the East Asian and the South Asian monsoons. It is governed by a subtropical humid monsoon climate, with dry and rainy seasons. There is a large distribution of terra rossa in Guizhou Province, ranging from a few centimeters to several meters in thickness. It is also found in cracks and between bedding surfaces of limestone and dolomite (Durn 2003; Feng et al. 2011). Study sites are located in Puchang in Suiyang County (PC), Xinpu in Zunyi (XP), Pingba County (PB) and Hezhang County (HZ). The sites PC and XP are located in the mid-north, PB is located in the mid-south, and HZ is located in the northwest (Fig. 1). The underlying bedrocks are Triassic limestone (PC), Upper–Middle Cambrian dolomites (XP), Lower Permian limestone (PB) and Early–Middle Triassic dolomites (HZ). The sampling sites are in a hilly area, and soil samples were taken from the terra rossa covering the hill pediment (Fig. 2).

Vegetation survey

A study of the vegetation at sites PC, XP and PB was conducted from 21 to 25 August 2011. The vegetation study at HZ took place on 10 October 2011. Both C_3 and C_4 plants were found at all sites. At the PC site, C_3 plants were mainly shrubs, and C_4 plants were mainly cultivated corn and *Artemisia scoparia*. At XP, C_3 plants were mainly *Ligustrum lucidum* and shrubs, and C_4 plants were mainly cultivated corn, *A. scoparia* and *Kobresia*. At PB, C_3 plants were mainly cultivated *Pinus massoniana*, *Eucommia ulmoides* and naturally growing *Pteridium aquilinum* and shrubs. The C_4 plants were mainly *Miscanthus floridulus*. At HZ, C_3 plants were mainly *P. massoniana* and shrubs, and C_4 plants mainly *Imperata cylindrica.*

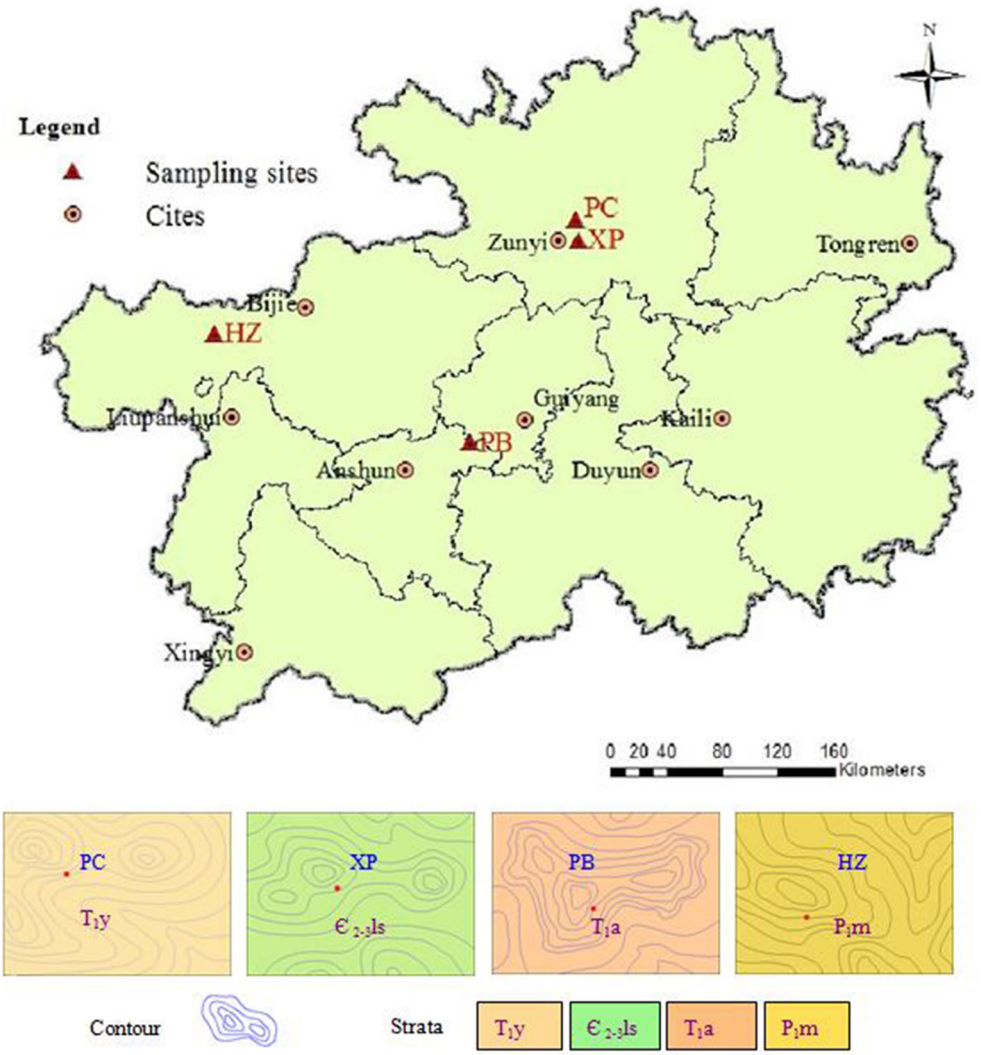

Fig. 1 Location, strata and altitude of study sites in Guizhou Province. *Red triangles* indicate the locations where the soil profiles were sampled. T_1y Triassic limestone, $\epsilon_{2\text{-}3}ls$ Upper–Middle Cambrian dolomites, P_1m lower Permian limestone, T_1a Early–Middle Triassic dolomites

Sample collection

Soil profiles were obtained by digging from the bottom to the top and were classified by soil color, texture, major element content (unpublished) and the soil horizon characteristics (Table 1). The soils were collected using a hand hammer and a small shovel, and were sampled at different intervals depending on the profile depth and the soil property. The PC soil was sampled at 20-cm intervals. The XP and PB soils were sampled at 10-cm intervals, and the HZ soil was sampled at 20-cm intervals in the clay layer and at 10-cm intervals in the loam layer. When a distinct change appeared in the soil color or texture, samples were not taken at intervals but by removing the soil with different characteristics. A soil sample of vertical 5 cm width was randomly collected from each horizon. The geological map of Guizhou Province was used to identify the parent material in the field. Each parent rock was identified by its texture, structure, shape and color, and being composed of at least three rock fragments.

Soil analyses

Soil samples were dried in the oven at 45 °C for 2 days, and a section of each was ground to pass a sieve (mesh 200). The unground soils were used for microscopic study. The soil particles were fixed on conductive tape, coated with carbon and studied using a scanning electron microscope and energy dispersive analysis of X-rays (SEM-EDAX) of JEOL JSM-6460LV, Japan. The mineral composition of the soil was analyzed using X-ray diffraction (XRD). Soil pH value was determined using a glass electrode in a 1:5 (volume fraction) suspension of soil in water (ISO 2005). Soil organic carbon (SOC) content was determined at the Environmental Pollution Control Laboratory at the Capital Normal University at Beijing, China. After acid-fuming to remove inorganic carbonate, the organic carbon in soil was converted to CO_2 by combustion with an Elementar Analysensysteme GmbH, Germany. The SOC content was calculated based on the amount of CO_2

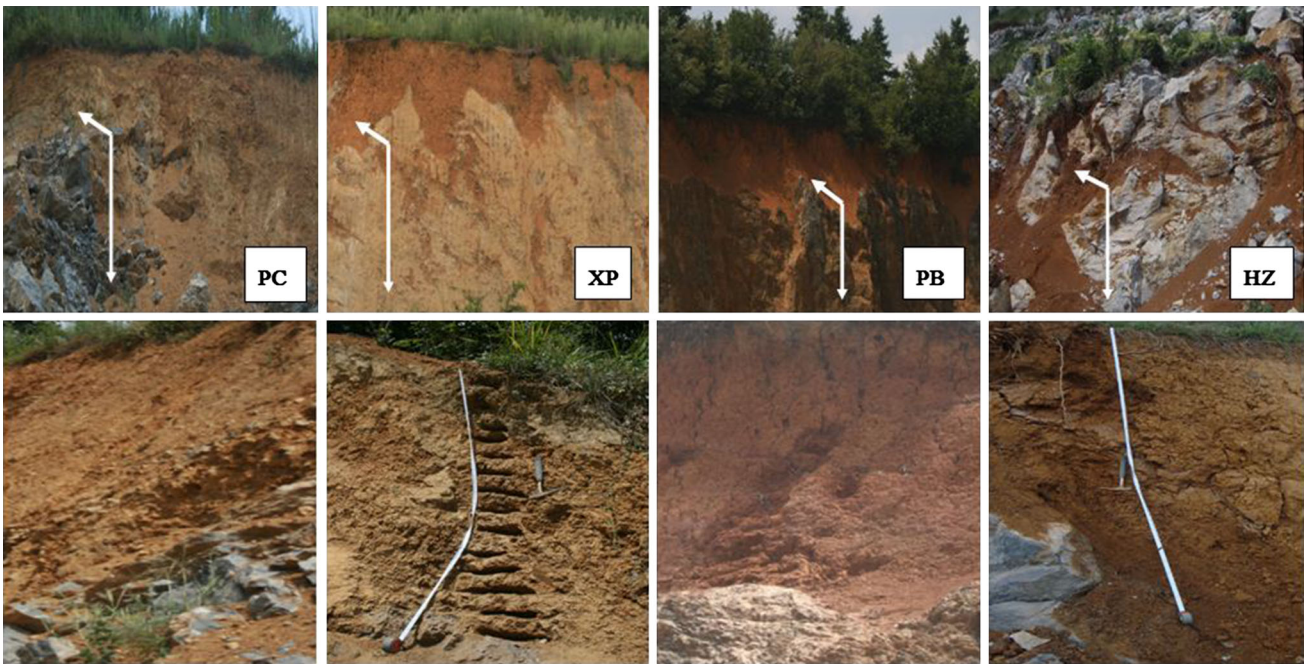

Fig. 2 The geomorphological characteristics of sampling sites

(Zhu and Liu 2006). The carbonate content in soil was determined by titrating 1 g of bulk samples using hydrochloric acid (1 mol/L) and sodium hydroxide (1 mol/L) (Cailleau et al. 2005).

Soil samples for organic C isotope analysis were pre-treated with 1 mol/L HCl to remove carbonate minerals. The sample residues were washed with distilled water and dried in the oven at 60 °C. Approximately 10–100 mg of treated sample was mixed with CuO and placed into a quartz tube. After combustion at 850 °C for 5 h, CO_2 was released (Boutton 1983). To measure stable C and O isotope composition of the soil carbonate, approximately 1.0–3.0 g of soil was heated at 350 °C in a muffle furnace for 3 h to pyrolyze organic C (Connin et al. 1997). This was then placed into an ampoule, capped and reacted with H_3PO_4 (100 %) for 1 day at room temperature (20–25 °C) (McCrea 1950). A sample of 50 mg carbonate rocks was directly reacted with H_3PO_4 (100 %) without pre-treatment. The released CO_2 was collected, cryogenically purified and measured with a mass spectrometer MAT252, Germany. The isotopes were analyzed and measured at the Institute of Geochemistry, Chinese Academy of Sciences. Carbonate and organic matter isotopic results are reported using standard δ (per mil, ‰) notation relative to the Pee Dee Belemnite standard. Precision of repeated standards was <0.04 ‰ for $\delta^{13}C$ and <0.09 ‰ for $\delta^{18}O$. Several soil samples were sent to Xian accelerator mass spectrometry center (XAAMS) for ^{14}C dating of soil organic carbon by accelerator mass spectrometry, AMS (Wallace et al. 1987). The ^{14}C data can be expressed as pMC (percent modern carbon) and $\Delta^{14}C$(‰) (Stuiver and Polach 1977). The ^{14}C age is calculated from the pMC (Stuiver and Polach 1977). When the $\Delta^{14}C < 0$, the turnover rate of soil organic matter is calculated from the equation inferred by Trumbore (1997) and Metting et al. (1999). When the $\Delta^{14}C > 0$, the turnover rate of soil organic matter is calculated based on the mathematical model developed by Cherkinsky and Borvkin (1993).

Results

Soil properties

The regolith is an expression of upward increase in weathering intensity. At the PC site, there is no obvious clay layer, and the clay stones are mixed with soil and increased with depth. At the XP and HZ site, the clay layer and soil layer are apparent, with clay layer observed in depths of >30 cm at XP and >80 cm at HZ. The plasticity of clay increases with depth, and the color changes between different layers (Table 2). At the PB site, the soil structure does not change with depth, but color changes at the depth of 150 cm (Table 2).

The pH value of the soil profiles shows that the soil changed from acidic to neutral from surface to depth. The pH value range is 6.1–8.4 at PC, 6.2–8.2 at XP, 5.3–7.4 at PB and 6.7–7.8 at HZ (Table 2).

The highest SOC content is observed in the surface soil at PC, XP and PB, and the SOC content decreases to <1 %

Table 1 Geomorphological and climatic information of the soil profile

Profile name	Type of soil (Chinese/US/FAO)	Longitude	Latitude	Type of bedrock	Elevation (m)	Mean annual temperature (°C)	Mean annual precipitation (mm/year)	Rainy seasons	Proportion of summer half year precipitation in annual precipitation (%)
PC	Cambisols/inceptisols/cambisols	107°02′30.7″	27°51′53.2″	Triassic limestone	951	15	1160	April to October	76.8
XP	Argosols/alfisols/acrisol	107°03′37.4″	27°44′2.8″	Upper–middle cambrian dolomites	853	13	1160	April to October	76.8
PB	Ferralsols/oxisols/ferralsols	106°21′42.5″	26°25′57.8″	Early–middle triassic dolomites	1256	18	1298	April to October	78.9
HZ	Argosols/alfisols/acrisol	104°43′27.5″	27°08′9.2″	Lower permian limestone	1689	12	927	May to September	81.8

from the surface to depth and remained almost stable at depth (Table 2). A similar trend was observed at HZ; however, the highest SOC content is found in the subsurface layer (10 cm depth). The depth distribution of organic carbon content is consistent with some previous studies (Zhu and Liu 2006; Li et al. 2009) and is closely related to the evolution of the soil profile (Chen et al. 2005) and the amount and activity of microbes (Zhu and Liu 2006).

The carbonate content is 4.0–9.5 % at PC, 2.5–12.5 % at XP, 8.0–16.5 % at PB and 5.5–17.5 % at HZ (Table 2). The carbonate content would increase with depth when considering the downward migration caused by precipitation, the increased pH value and the decreased weathering degree of carbonate rocks at the deeper depth. In fact, it shows an irregular variation with depth, and the carbonate content in the surface soil is higher than the average value of the whole profile (PC 9.5 % surface vs. 6.9 % average; XP 10.0 % surface vs. 8.2 % average; PB 11.8 % surface vs. 11.2 % average; HZ 16.0 % surface vs. 12.5 % average).

Morphology and distribution of calcretes

Most of the carbonates in this study are characterized microscopically by features similar to pedogenic carbonates. They are poorly crystallized with structures resembling root or vessels of plant tissues (Fig. 3a–c, e, f) or occurs as calcitic coatings on soil matrix mixed with root (Fig. 3d). These carbonates with pedogenic features take the main form in SEM study, and most often, they are found in the shallow soil horizon. Carbonate cements (Fig. 3i) are sometimes found at the deeper depth. Almost all of the carbonates occur as calcrete in proximity to clay (Fig. 3), sometimes with a clay coating covering around the carbonate (Fig. 3b), and the carbonate also occur with several minerals including quartz, feldspar, smectite, illite and kaolinite.

Stable carbon isotopic composition of soil organic matter ($\delta^{13}C_{SOM}$)

There is a great vertical variation of $\delta^{13}C_{SOM}$ at each site (Table 2). Most $\delta^{13}C_{SOM}$ are in the range of C_3 plants (−32 to −21 ‰), and only a few are in the range of C_4 plants (−17 to −9 ‰) (Landi et al. 2003). At the PC site, most samples are in the C_3 plant range; values at depths of 70, 110 and 210 are in the C_4 plant range. Value at 10 cm is neither in the C_3 nor C_4 plant range, which may be the result of a mixture of C_3 and C_4 plants. At the XP site, the topsoil has an abnormally high $\delta^{13}C_{SOM}$ value (−10.91 ‰) compared with other sites. Below the surface, the $\delta^{13}C_{SOM}$ increases from −24.93 ‰ at 5 cm to −20.66 ‰ at 20 cm and then remained nearly constant at around −24.00 ‰. At the PB site, most samples are in the C_3 plant range. Values

Table 2 Soil properties and stable isotopic values of soil organic matter and disseminated carbonate

Sample sites	Depth (cm)	Musell colors of dry soil	Soil texture	SOC content (% C)	Carbonate content (%)	$\delta^{13}C_{SOM}$ (‰)	$\delta^{13}C_{SC}$ (‰)	$\delta^{18}O_{SC}$ (‰)	pH
PC-1	0	10 year 4/4, dark yellow brown	Sandy loam	2.33	9.5	−25.15	−10.36	−14.68	6.8
PC-2	10	10 year 5/8, yellowish brown	Sandy loam	0.52	7.5	−18.29	−16.81	−17.91	6.2
PC-3	30	10 year 5/8, yellowish brown	Sandy soil	0.35	7.8	−23.42	−18.79	−16.74	6.1
PC-4	50	10 year 6/6, brownish yellow	Sandy soil	0.30	7.0	−24.16	−17.82	−18.88	6.2
PC-5	70	10 year 6/8, brownish yellow	Sandy soil	0.39	8.0	−14.46	−17.24	−16.09	6.4
PC-6	90	10 year 6/8, brownish yellow	Sandy soil	0.31	9.0	−25.01	−17.55	−15.51	6.6
PC-7	110	10 year 6/8, brownish yellow	Sandy soil	0.32	4.0	−15.08	−17.12	−15.63	6.7
PC-8	130	10 year 6/8, brownish yellow	Sandy soil	0.37	5.0	−24.42	−16.23	−13.22	7
PC-9	150	10 year 6/8, brownish yellow	Sandy soil	0.30	7.0	−24.11	−14.82	−15.30	7.2
PC-10	170	10 year 7/8, yellow	Sandy soil	0.29	9.0	−24.57	−8.42	−12.59	7.3
PC-11	190	10 year 7/8, yellow	Sandy soil	0.27	4.5	−24.51	−13.71	−15.58	7.7
PC-12	210	10 year 6/8, brownish yellow	Sandy soil	0.19	4.0	−13.60	−16.14	−16.24	8
XP-1	0	10 year 3/4, dark yellowish brown	Light loam	2.68	10.0	−10.91	−15.23	−13.10	6.2
XP-2	5	10 year 4/4, dark yellowish brown	Sandy loam	2.03	7.0	−24.93	−15.28	−12.98	6.6
XP-3	10	10 year 4/6, dark yellowish brown	Sandy loam	0.72	10.5	−21.57	−14.17	−15.43	6.6
XP-4	20	10 year 5/4, yellowish brown	Sandy loam	0.66	7.5	−20.66	−15.35	−14.72	6.5
XP-5	30	10 year 7/6, yellow	Clay	0.41	8.5	−24.32	−12.85	−14.21	6.4
XP-6	40	10 year 6/8, brownish yellow	Clay	0.35	9.5	−24.01	−14.81	−13.06	6.5
XP-7	50	10 year 6/8, brownish yellow	Clay	0.4	8.5	−23.76	−14.35	−11.81	6.5
XP-8	60	10 year 7/8, yellow	Clay	0.43	11.0	−24.30	−11.54	−14.60	6.7
XP-9	70	10 year 8/6, yellow	Clay	0.38	10.5	−24.55	−16.87	−13.65	6.7
XP-10	80	10 year 8/6, yellow	Clay	0.38	8.0	−24.79	−14.94	−14.31	6.8
XP-11	90	10 year 6/8, brownish yellow	Clay	0.37	9.5	−24.20	−15.02	−13.78	6.9
XP-12	100	10 year 7/8, yellow	Clay	0.48	12.5	−22.50	−15.52	−13.75	7.5
XP-13	110	10 year 8/6, yellow	Clay	0.4	4.0	−24.00	−14.14	−12.33	7.3
XP-14	120	10 year 7/8, yellow	Clay	0.54	2.5	−24.27	−10.64	−11.31	7.8
XP-15	130	10 year 7/6, yellow	Clay	0.95	4.0	−24.59	−6.86	−9.61	8.2
PB-1	20	7.5 year 6/8, reddish yellow	Sandy loam	1.05	11.8	−22.04	−13.61	−12.05	5.3
PB-2	30	7.5 year 6/8, reddish yellow	Sandy loam	0.75	9.0	−19.87	−15.40	−17.25	5.6
PB-3	40	7.5 year 6/8, reddish yellow	Sandy loam	0.61	8.8	−20.24	−12.66	−9.54	5.9
PB-4	50	7.5 year 7/8, reddish yellow	Sandy loam	0.55	8.2	−22.76	−13.80	−11.11	6.1
PB-5	60	7.5 year 7/8, reddish yellow	Sandy loam	0.54	8.0	−22.26	−10.86	−10.47	5.9
PB-6	70	7.5 year 6/8, reddish yellow	Sandy loam	0.48	14.0	−22.33	−9.28	−11.41	6
PB-7	80	7.5 year 7/8, reddish yellow	Sandy loam	0.44	16.5	−22.44	−5.93	−10.61	6.3
PB-8	90	7.5 year 7/8, reddish yellow	Sandy loam	0.36	13.3	−15.20	−8.83	−9.41	6.5
PB-9	100	7.5 year 7/8, reddish yellow	Sandy loam	0.33	14.5	−23.25	−10.78	−11.81	6.9
PB-10	110	7.5 year 6/8, reddish yellow	Sandy loam	0.41	9.0	−23.19	−10.11	−11.27	6.9
PB-11	120	7.5 year 7/8, reddish yellow	Sandy loam	0.4	10.5	−22.73	−9.85	−10.09	7
PB-12	130	7.5 year 7/8, reddish yellow	Sandy loam	0.46	8.5	−24.67	−10.46	−11.59	7
PB-13	140	7.5 year 6/8, reddish yellow	Sandy loam	0.45	10.0	−17.89	−11.24	−12.66	7.1
PB-14	150	7.5 year 6/8, reddish yellow	Sandy loam	0.45	9.0	−20.59	−12.69	−11.94	7.1
PB-15	160	7.5 year 5/8, strong brown	Sandy loam	0.39	12.5	−13.27	−13.03	−13.30	7.1
PB-16	170	7.5 year 4/6, strong brown	Sandy loam	0.36	12.5	−22.65	−12.87	−13.25	7.1
PB-17	180	7.5 year 4/6, strong brown	Sandy loam	0.36	14.3	−16.54	−13.07	−14.13	7.4
HZ-1	0	10 year 4/6, dark yellowish brown	Light loam	0.78	16.0	−25.92	1.31	0.67	7.6
HZ-2	10	10 year 5/8, yellowish brown	Light loam	3.03	14.0	−20.94	−10.88	−2.58	6.9
HZ-3	20	10 year 5/8, yellowish brown	Light loam	1.37	17.5	−21.68	−11.46	−2.48	6.7

Table 2 continued

Sample sites	Depth (cm)	Musell colors of dry soil	Soil texture	SOC content (% C)	Carbonate content (%)	$\delta^{13}C_{SOM}$ (‰)	$\delta^{13}C_{SC}$ (‰)	$\delta^{18}O_{SC}$ (‰)	pH
HZ-4	30	10 year 5/6, yellowish brown	Light loam	1.05	10.0	−30.45	−12.34	−2.89	6.7
HZ-5	40	10 year 5/6, yellowish brown	Light loam	0.77	10.5	−22.80	−13.15	−3.12	6.7
HZ-6	50	10 year 5/6, yellowish brown	Light loam	0.56	9.5	−22.80	−10.52	−3.08	6.8
HZ-7	60	10 year 5/8, yellowish brown	Light loam	0.39	5.5	−24.38	−6.97	−1.00	6.9
HZ-8	80	10 year 5/8, yellowish brown	Clay	0.51	11.5	−23.37	−11.41	−1.46	7
HZ-9	100	10 year 6/8, brownish yellow	Clay	0.52	12.0	−24.75	−9.55	−0.46	7.2
HZ-10	120	10 year 6/8, brownish yellow	Clay	0.49	15.0	−24.51	−9.56	−0.55	7.6
HZ-11	140	10 year 5/8, yellowish brown	Clay	0.65	13.0	−24.13	−8.99	0.4	7.3
HZ-12	160	10 year 6/8, brownish yellow	Clay	0.55	13.0	−25.56	−8.07	0.09	7.1
HZ-13	180	10 year 3/6, dark yellowish brown	Clay	1.04	14.0	−22.66	−3.12	1.84	7.5
HZ-14	200	10 year 4/6, dark yellowish brown	Clay	0.86	12.0	−13.41	−2.69	0.87	7.6
HZ-15	220	10 year 4/6, dark yellowish brown	Clay	1.00	13.5	−25.51	1.08	3.33	7.8

at depths of 110, 160, 180 and 200 are in the C_4 plant range, and values at 50, 60 and 170 are neither C_3 nor C_4 plants. At the HZ site, the $\delta^{13}C_{SOM}$ value first increases from −25.92 ‰ at the surface to −20.94 ‰ at 10 cm depth and decreases to −25.51 ‰ at 220 cm. During this decrease, there was a large negative and positive offset at 30 cm and 200 cm with $\delta^{13}C_{SOM}$ values of −30.45 and −13.41 ‰, respectively.

Stable carbon and oxygen isotopic composition of soil carbonate ($\delta^{13}C_{SC}$ and $\delta^{18}O_{SC}$)

The $\delta^{13}C_{SC}$ at PC ranges from −8.42 to −18.79 ‰, with an average of −15.42 ‰. The $\delta^{13}C_{SC}$ at XP ranges from −16.87 to −6.86 ‰, with an average of −13.84 ‰. The $\delta^{13}C_{SC}$ at PB ranges from −15.40 to −5.93 ‰, with an average of −11.44 ‰. The $\delta^{13}C_{SC}$ at HZ ranges from −13.15 to 1.31 ‰, with an average of −7.75 ‰ (Table 2). The order of the average $\delta^{13}C_{SC}$ between the sites is HZ > PB > XP > PC.

The $\delta^{18}O_{SC}$ at PC ranges from −18.88 to −12.59 ‰, with an average of −15.70 ‰. The $\delta^{18}O_{SC}$ at XP ranges from −15.43 to −9.61 ‰, with an average of −13.24 ‰. The $\delta^{18}O_{SC}$ at PB ranges from −17.25 to −9.41 ‰, with an average of −11.88 ‰. The $\delta^{18}O_{SC}$ at HZ ranges from −3.12 to 3.33 ‰, with an average of −0.70 ‰ (Table 2). The order of the average $\delta^{18}O_{SC}$ between the sites is HZ > PB > XP > PC (Table 2).

The $\delta^{13}C_{SC}$ and $\delta^{18}O_{SC}$ from the depths >50 cm at each site show a positive relationship with different correlation coefficient (Fig. 4). Values of depths >50 cm were chosen because they are less likely to be impacted by atmospheric CO_2 and may reflect $\delta^{13}C$ composition of CO_2 derived from soil respiration (Quade et al. 2007). The $\delta^{13}C_{SC}$ values (y, in ‰) are related to $\delta^{18}O_{SC}$ values (x, in ‰) as follows:

$$y = 1.0945x + 1.4587\left(\mathrm{PC}, R^2 = 0.4459\right)$$

$$y = 1.346x + 3.9044\left(\mathrm{XP}, R^2 = 0.5132\right)$$

$$y = 1.1867x + 3.227\left(\mathrm{PB}, R^2 = 0.6245\right)$$

$$y = 2.4824x - 7.4329\left(\mathrm{HZ}, R^2 = 0.8197\right).$$

The stable carbon and oxygen isotopic composition of the parent carbonate rocks is 2.55 ‰ ($\delta^{13}C$) and −6.92 ‰ ($\delta^{18}O$) at PC, −1.71 ‰ ($\delta^{13}C$) and −7.7 ‰ ($\delta^{18}O$) at XP, 1.2 ‰ ($\delta^{13}C$) and −1.09 ‰ ($\delta^{18}O$) at PB, 3.39 ‰ ($\delta^{13}C$) and −10.07 ‰ ($\delta^{18}O$) at HZ.

Carbon radioisotopic data of soil organic matter

The pMC and $\Delta^{14}C$ is, respectively, <100 and <0 except for that of the surface soil at XP (Table 3). When the pMC > 100 or $\Delta^{14}C > 0$, it means great influence of bomb ^{14}C caused by the nuclear test since 1956, and the ^{14}C age of SOM is modern and cannot be directly determined, such as the surface soil at XP (XP-1) (Table 3). The carbon radioisotopes of soil organic matter show an increased age of organic matter with depth except that at XP. The organic carbon at 130 cm (XP-15) is younger than that at 80 cm (XP-10) (Table 3), which may be caused by mixing of younger organic residues. Supposed the modern age of XP-1is 55 years since the bomb (Table 3), the dating results and the soil depths have a good linear relationship (Fig. 5). The regression equations in Fig. 5 are used to estimate the age of SOM in other soil layers according to their depth (Fig. 6). The estimated age in Fig. 6 only shows an approximate age variation with depth but not the actual age

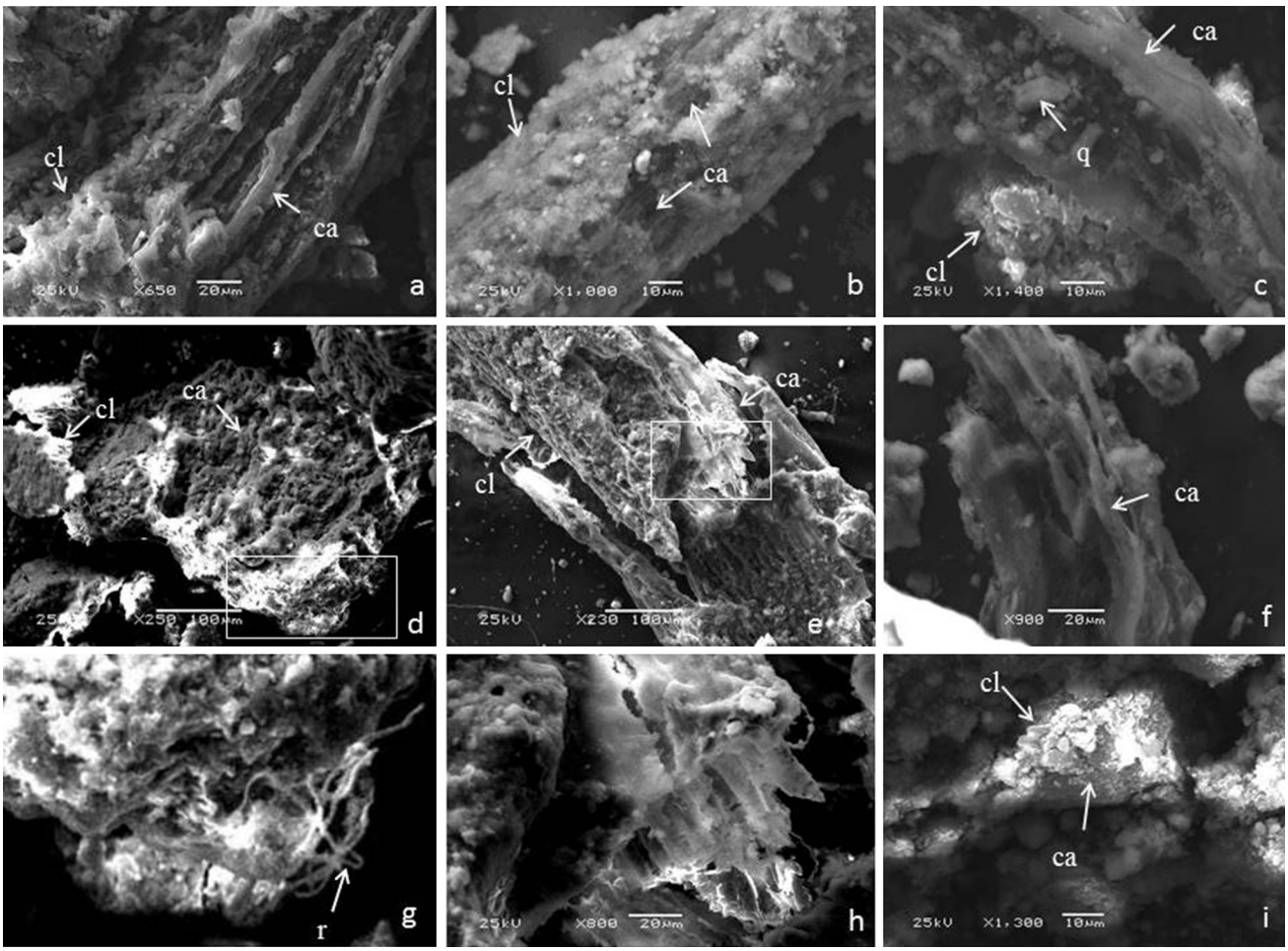

Fig. 3 SEM micrographs of carbonate in soil (**a**–**i**). **a** *Root-shaped* carbonate filled with soil matrix and clay from the surface soil PC–1; cl—clay, ca—carbonate. **b** Calcified root hair with clay coating covered around from PC–2, 10 cm from the surface soil; cl—clay, ca—carbonate. **c** *Root-shaped* carbonate with inclusion of clay minerals and quartz from PC–3, 30 cm from the surface soil; cl—clay, ca—carbonate, q—quartz. **d** Calcitic coatings on soil matrix mixed with roots from surface soil XP–1; cl—clay, ca—carbonate. **e** Carbonate structures resembling vessels of plant tissues with clay around from XP–2, 5 cm from the surface soil; cl—lay, ca—carbonate. **f** Calcified plant tissues from PB–3, 40 cm from the surface soil; ca—carbonate. **g** Fragment marked by frame in *panel d*, partial detail of root; r—root. **h** Fragment marked by frame in *panel e*, the enlarged carbonate structure. **i** Coarse cemented carbonate with clay coatings from HZ–15, 220 cm from the surface soil; cl—clay, ca—carbonate

in each layer considering other factors that may affect the age of SOM, such as the pedoturbation of SOM caused by biological activities or mixing of organic materials of other periods.

The turnover rate of SOM at each profile decreases with depth (Table 3), reflecting a formation and update regularity of organic matter in the soil profiles. According to the turnover rate, the organic carbon of surface soil at XP (XP-1) is active carbon, and that of other soil samples are stable carbon. Compared with the radioisotopic research about the forest soil in southern China (Xing 1998), the $\Delta^{14}C$ value of a certain depth in this study is smaller than that of the same depth in forest soil, indicating a longer timescale of soil carbon storage in this studied soil.

Discussion

Origin of carbonate in terra rossa

Terra rossa is generally defined as a type of reddish to silty clay deposit over carbonate bedrock (Durn 2003; Feng et al. 2011). Most researchers today believe that terra rossa is a polygenetic relict soil formed during the Tertiary and/or hot and humid periods of the quaternary (Altay 1997; Bronger and Bruhn 1997). In some isolated karst terrain, terra rossa may have formed exclusively from the insoluble residue of limestone and dolomite, but more often, it comprises a range of parent materials (Durn et al. 1999). Several studies of terra rossa in Guizhou Province have concluded that it is a product of in situ weathering that

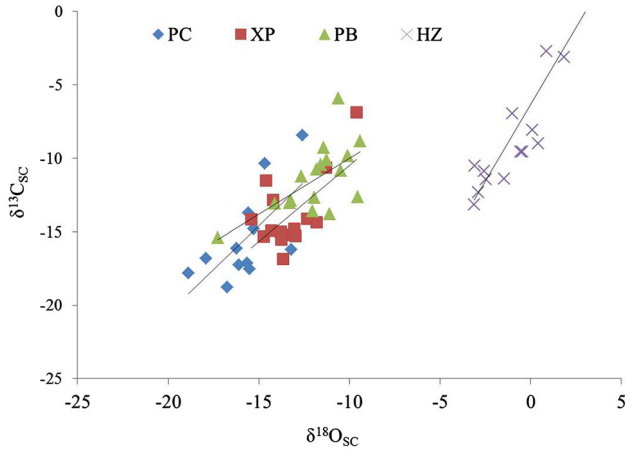

Fig. 4 Relationship between stable carbon and oxygen isotopes of soil carbonate ($\delta 13C_{SC}$ and $\delta 18O_{SC}$) from >50 cm depth

originated mostly from the insoluble residues of the parent rocks (Feng et al. 2009a, b; Ji et al. 2004a, b; Wei et al. 2013; Li and Ji 2015). The formation process of terra rossa can be divided into two stages, the weathering reaction mainly happened at the first stage in rock–regolith interface, with almost completely leaching of Ca and Na and accumulation of Al. The second stage is the accumulation and further weathering of the insoluble residua (Ji et al. 2004a, b). Therefore, the carbonate in terra rossa may contain pedogenic and lithogenic carbonates. Pedogenic carbonates usually occur in arid and semiarid areas (Kovda et al. 2006; Achyuthan et al. 2007; Quade et al. 2007); it appears that both pedogenic and lithogenic carbonates are easily leached out in slightly acidic soil environment with high rainfall (Table 1).

In this study, macroscopic carbonates were hardly found in soil, whereas the carbonates were observed in SEM study as the disseminated calcrete in soil (Fig. 3). Based on the photomicrographs, most carbonates are poorly crystallized and characterized by distinct biogenic structures (Fig. 3). The root-shape calcrete (Fig. 3a–c), calcitic coatings on soil matrix mixed with root (Fig. 3d) and calcitic structures resembling vessels of plant tissues (Fig. 3e, f). These carbonate structures demonstrate biogenetic processes and indicate their pedogenic origin. The carbonate with pedogenic features was more commonly found at the shallow soil horizons with strong biological activity, rather than in the deeper horizons that, considering the physicochemical conditions, are more favorable for the precipitation of carbonate. This is in accordance with higher surface carbonate content than the average value at each profile. This means that the physicochemical conditions, including the downward migration caused by precipitation and the higher pH value at the deeper horizons (Table 2), do not yield a close correlation with the presence of carbonate in this study. The photomicrographs of the carbonates clearly showed the impact of plant and root in the formation of pedogenic carbonates. Some studies have discussed the impact of the rhizosphere in the formation of pedogenic carbonates, which is related to two main processes: acceleration of carbonate parent material dissolution by the organic acids excreted by roots and precipitation of secondary calcium carbonate due to water losing by root pumping or through the root channel (Becze-Deak et al. 1997). Whether the first process plays an important role in this study is unknown considering the already strong water–rock interaction in karst area, but the second process such as the cementation process, impregnation by secondary calcium carbonate of the soil around root traces, can explain why the pedogenic carbonates have the shape of roots (Fig. 3a–c) and appear at the rhizosphere

Table 3 Carbon radioisotopes and ^{14}C age of soil organic matter

Sample number	Soil depth (cm)	pMC (%)	$\Delta^{14}C$ (‰)	Turnover rate of SOM (a^{-1})	^{14}C age of SOM (a BP)
PC-14	0	82.99	−170.1	6.07E−04	1498
PC-13	10	45.09	−549.1	1.02E−04	6399
PC-7	130	28.71	−712.9	5.01E−05	10025
XP-18	0	104.75	47.5	9.96E−01	Modern
XP-15	20	88.48	−115.2	9.56E−04	983
XP-9	80	48.13	−518.7	1.16E−04	5875
XP-4	130	57.33	−426.7	1.67E−04	4470
PB-20	20	74.61	−253.9	3.66E−04	2353
PB-12	100	31.94	−680.6	5.84E−05	9169
PB-6	160	22.78	−772.2	3.67E−05	11885
HZB-16	0	74.26	−257.4	3.59E−04	2390
HZB-13	30	60.08	−399.2	1.87E−04	4093
HZB-6	140	7.69	−923.1	1.04E−05	20605

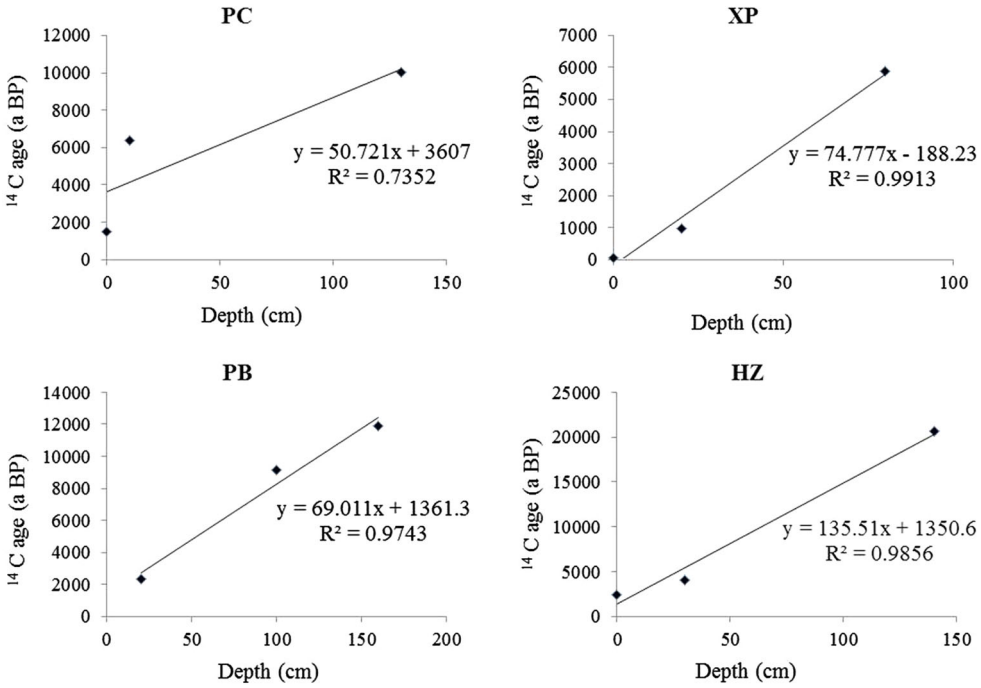

Fig. 5 Relationship between ^{14}C age of soil organic matter and soil depth

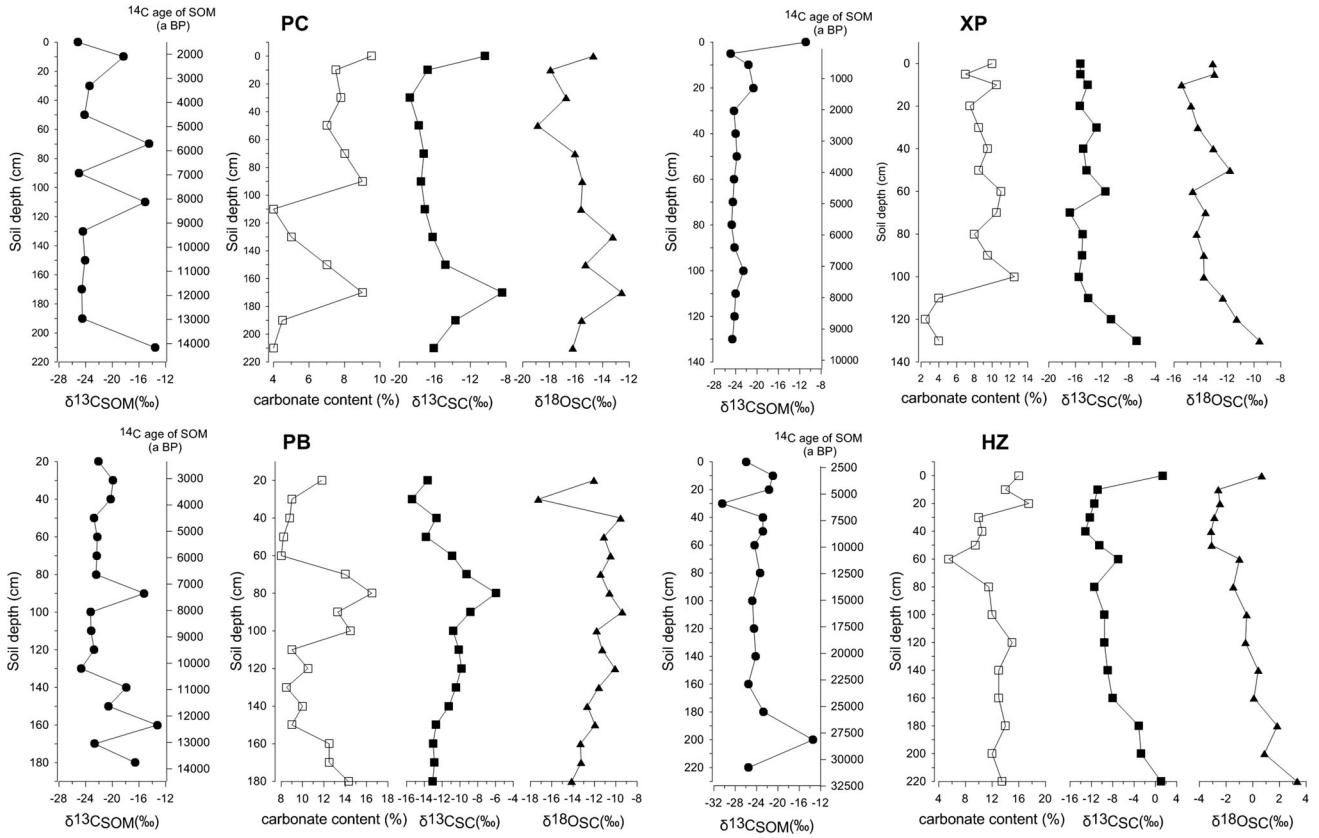

Fig. 6 Depth distributions of stable carbon isotopes of soil organic matter ($\delta^{13}C_{SOM}$) and the corresponding ^{14}C age in each layer. Depth distributions of carbonate content, stable carbon and oxygen isotopes of soil carbonate ($\delta^{13}C_{SC}$ and $\delta^{18}O_{SC}$)

(Fig. 3d). Not only do roots promote the precipitation of secondary calcium carbonate around them, but they also absorb calcium. Some plants have the ability to accumulate $CaCO_3$ in their vacuome in order to detoxify a possible excess of Ca^{2+} (Verrecchia 2011). The biomineralization then resulted in the calcified plant tissues (Fig. 3e, f). Few pedogenic carbonate structures are found in the soils at deeper depth (about >40 cm). Very few coarse hardened carbonate occur, such like that in the clay layer that lies on the parent rock at the HZ site (Fig. 3g). Its origination is still unclear, which may have formed by re-precipitation of the dissolved carbonate with consequent induration or cementation or originated from the carbonate detritus that was not completely weathered.

Based on the elementary analysis of SEM-EDAX, few carbonate structures are composed of pure $CaCO_3$, most are with the inclusion of Al, Si and Fe. According to XRD results, the Al and Si are derived from clay minerals or quartz; the Fe is derived from the iron minerals. Almost all of the carbonate is composed of calcrete associated with clay (Fig. 3), and sometimes with clay coating almost conceals and protects the carbonate within (Fig. 3b). The clay materials therefore may play a role in preventing the leaching of carbonate that was packed inside. Though clay content was not determined in laboratory, the field observations show that the clay content is higher in deeper soil depth (Table 2); this may explain the absence of carbonate structure in SEM study for soil at deeper depth, because the clay wrapped the carbonate inside and put the carbonate out of sight. Royer indicated that the soil parent material and texture both play a role in the formation of the carbonate, especially when the parent materials are dominated by calcium carbonate and the soil texture and is dominated by sand, silt, or clay (Royer 1999). To further differentiate pedogenic carbonates from lithogenic carbonates, stable isotopic analysis of soil carbonate is needed. The $\delta^{13}C_{SC}$ values at the four sites are all within the range of pedogenic carbonates (Cerling 1984; Quade et al. 1989; Monger et al. 1998), confirming that the disseminated carbonate is mainly composed of pedogenic carbonates in the studied soil.

Interpretation of $\delta^{13}C_{SOM}$

Based on previous research findings (Farquhar et al. 1989; Buchmann et al. 1997; Boutton et al. 1998), the inherent carbon isotope fractionation process in the soil profile usually causes the $\delta^{13}C_{SOM}$ value to vary within a range of 1–3 ‰. If the change is >3 ‰, it demonstrates that the soil substances were the mixture of C_3 and C_4 plants. The $\delta^{13}C_{SOM}$ variation at each site all exceeds 3 ‰. The changes of greater than 3 ‰ between adjacent sampling layers are counted, and the results show that 3 of 7 great changes are accompanied with the change in soil color for PC, 3 of 3 for XP, 3 of 6 for PB and 3 of 5 for HZ. A few $\delta^{13}C_{SOM}$ changes of greater than 3 ‰ are accompanied with the changes in soil texture, such as that from the depth of 10 to 30 cm at PC. That from 0 to 5 cm, 20 to 30 cm at XP is accompanied with the changes in both soil color and soil texture (Table 2). Not all changes in soil color are accompanied with great change in $\delta^{13}C_{SOM}$. The changes in soil texture from upper layer to lower layer at PC and XP are accompanied with a great decrease in $\delta^{13}C_{SOM}$ (Table 2). The results suggest certain connection may exist between the $\delta^{13}C_{SOM}$ and the soil properties.

Plants with C_3 and C_4 photosynthesis have unique $\delta^{13}C$ values, which are not significantly altered during decomposition and soil organic matter formation (Boutton et al. 1998). Consequently, the $\delta^{13}C$ of soil organic matter reflects the relative contribution of C_3 and C_4 plants. The relative percentage of soil organic matter derived from C_3 and C_4 plants was calculated using the following formula (Landi et al. 2003):

$$\text{Percentage of } C_3 \text{ plants} = \frac{\delta^{13}C_{SOM} - \delta^{13}C_4}{\delta^{13}C_3 - \delta^{13}C_4} \quad (1)$$

where $\delta^{13}C_{SOM}$ is the $\delta^{13}C$ of soil organic matter, $\delta^{13}C_3$ is the average $\delta^{13}C$ of C_3 plants (−27 ‰) and $\delta^{13}C_4$ is the average $\delta^{13}C$ of C_4 plants (−13 ‰).

The percentage calculated from $\delta^{13}C_{SOM}$ show that C_3 plants account for a larger proportion than C_4 plants at each site in different degrees (Fig. 7). At PC, about 2/3 of the soil layers show a dominance of C_3 plants. At XP, the organic matter originates entirely from C_4 plants at the surface, and more from C_3 plants below the surface. At PB, most of the samples are close to the fifty–fifty line. At HZ, soil organic matter at the depth of 200 cm originates mostly from C_4 plants, and the others originate mostly from C_3 plants.

Large increase in $\delta^{13}C_{SOM}$ is observed at each site at different depths (Fig. 6), such as the sample of 70, 110 and 210 at PC; the sample of 0 cm at XP; the sample of 90 and 160 cm at PB; the sample of 200 cm at HZ. Except for XP, other three profiles have positive shift of $\delta^{13}C_{SOM}$ to about −14 ‰, falling in the C_4 plant range, which can be seen as a signal of change into warm and dry in climate. This climate change happened at about 6000–8000 a BP and 12000–14000 a BP according to PC and PB, 28000 a BP according to HZ. The surface samples at XP decreased by approximately 14 ‰ from the surface to a depth of 5 cm. There have been no reports of climatic change that would have caused such a striking change at that period in Guizhou Province (Kuo et al. 2011). Based on the vegetation investigation, the modern age and the rapid turnover rate of the surface SOC at XP, the positive offset was most

likely caused by cultivation of corn which is a crop with short growing cycle.

It appears that the positive shifting samples have made the entire depth distribution of $\delta^{13}C_{SOM}$ irregular. If those felling in the C_4 plant range are excluded, the other points form a regular distribution along the depth axis (Fig. 6). According to previous research findings (Boutton et al. 1998; Nordt et al. 1998; Zhu and Liu 2006), the $\delta^{13}C_{SOM}$ values do not increase steadily with depth but instead reach a maximum value at a certain depth and then decrease gradually and remain almost stable. In this study, most samples at each site have much the similar trend from the topsoil to depth. Many papers have discussed the potential factors leading to the observed enrichment of ^{13}C with depth (Boutton et al. 1998; Ehleringer et al. 2000). These factors include higher $\delta^{13}C$ values of atmospheric CO_2 before the Industrial Revolution caused by the combustion of ^{13}C-depleted fossil fuels. Compared with the newly formed organic matter of topsoil, that in the deeper soil layers originated at a time when the $\delta^{13}C$ of atmospheric CO_2 was more positive and thus has a higher $\delta^{13}C$ value. Based on the ^{14}C age of the soil organic matter, this reason is excluded because except for the surface soil at XP, other surface soil organic matter is formed before Industrial Revolution. Other possible factors are ascribed to the microbial activities. Microorganisms preferentially use the carbon source of depleted ^{13}C during litter decomposition, causing the residual organic matter to become progressively more positive in its $\delta^{13}C$ values. The $\delta^{13}C$ values of the below ground biomass (roots) are higher compared with above ground biomass (leaves). Below 25 cm, the $\delta^{13}C$ values of SOM in soil decreased with depth, which usually is caused by the effects of microbial degradation. Microbial populations preferentially metabolize nutrient and energy-rich high-^{13}C compounds, such as polysaccharides, leaving the remaining SOM enriched in low-^{13}C and recalcitrant compounds, such as lignin (Wynn et al. 2006; Zhu and Liu 2006).

Interpretation of $\delta^{13}C_{SC}$ and $^{18}O_{SC}$

The changes in $\delta^{13}C_{SC} > 3$ ‰ between adjacent sampling layers are also counted, with 2 of 3 accompanied with the change in soil color for PC, 3 of 3 for XP, 1 of 1 for PB and 3 of 5 for HZ. A change in soil texture at HZ is accompanied with 4.44 ‰ decrease in $\delta^{13}C_{SC}$ (Table 2). The results suggest a closer connection between the change in $\delta^{13}C_{SC}$ and soil color compared with $\delta^{13}C_{SOM}$, indicating that the $\delta^{13}C_{SC}$ is more affected by the composition of soil.

The soil carbonate usually contains a mixture of lithogenic and pedogenic carbonate. As mentioned before, the stable carbon isotope of pedogenic carbonate in soil is predominantly set by the $\delta^{13}C$ value of soil CO_2. According to the stable C isotope diffusion model of Ceiling and Quade (Cerling 1984; Quade et al. 1989), at depths below the influence of the atmosphere, a $\delta^{13}C$ offset of approximately 15 ‰ exists between the soil organic matter and the pedogenic carbonate, which is the sum of approximately 4.4 and 11.0 ‰ originating from molecular diffusion of CO_2 and carbonate equilibrium reactions, respectively (Nordt et al. 1998). Therefore, the stable carbon isotope of pedogenic carbonate ($\delta^{13}C_{PC}$) is expressed as:

$$\delta^{13}C_{PC} = \delta^{13}C_{SOM} + \Delta CO_2 \text{ diffusion } + \Delta CO_2 - CaCO_3 \quad (2)$$

where the ΔCO_2 diffusion is the $\delta^{13}C$ difference between soil CO_2 and respired CO_2 caused by molecular diffusion, and the ΔCO_2–$CaCO_3$ is the $\delta^{13}C$ difference between C in $CaCO_3$ and CO_2 occurring during equilibrium reactions. In theory, the $\delta^{13}C_{SOM}$ is weighted for all horizons in the upper 25 cm (Nordt et al. 1998). A 25-cm depth is chosen because the organic matter content that produces CO_2 is the highest in the upper 20–30 cm zone and decreases appreciably below this depth (Nordt et al. 1998; Quade et al. 2007). This depth coincides with the modeled attenuation depth for CO_2 production in soils with a relatively high respiration rate (Cerling 1984; Quade et al. 1989). However, according to the $\delta^{13}C_{SOM}$ values discussed in Sect. 4.2, the $\delta^{13}C_{SOM}$ value of the upper 25 cm is not applicable for all sites. For example, the vegetation system has changed considerably at the surface at XP; hence, the $\delta^{13}C_{SOM}$ of the topsoil cannot be used to represent the actual $\delta^{13}C$ value of soil-respired CO_2 that contributed to pedogenic carbonate formation. The average $\delta^{13}C_{SOM}$ value of 0–30 cm at PC (−22.29 ‰), 5–20 cm at XP (−22.39 ‰), 20 cm at PB (−22.04 ‰) and 0–20 cm at HZ (−22.85 ‰) are therefore used to calculate the $\delta^{13}C_{PC}$ values. The estimated $\delta^{13}C_{PC}$ value is approximately −7 ‰ for all sites (Fig. 8). The estimated $\delta^{13}C_{PC}$ value is higher than the $\delta^{13}C_{SC}$ value in the same horizon for most layers, particularly at PC, XP and PB (Fig. 8). However, the $\delta^{13}C_{PC}$ value should be lower than the $\delta^{13}C_{SC}$, because the $\delta^{13}C_{SC}$ is the value of mixed lithogenic and pedogenic carbonate, and the $\delta^{13}C$ value of lithogenic carbonate is much higher than that of $\delta^{13}C_{PC}$. This unexpected finding illustrates that the C_3 plants made up a larger percentage of the vegetation during the time of carbonate precipitation.

The percentage of C_3 plants can also be calculated by replacing $\delta^{13}C_{SOM}$ in Eq. (1) with $\delta^{13}C_{SC}$. The corresponding $\delta^{13}C_3$ is the $\delta^{13}C$ value of C_3 carbonate (−12 ‰), and $\delta^{13}C_4$ is the $\delta^{13}C$ value of C_4 carbonate (2 ‰) (Connin et al. 1997). The percentage of C_3 plants calculated by $\delta^{13}C_{SC}$ at PC, XP and PB was higher than that calculated by $\delta^{13}C_{SOM}$ (almost 100 % at PC and XP) (Fig. 7), further supporting that C_3 plants made up a larger percentage when carbonate precipitated. The percentage calculated by

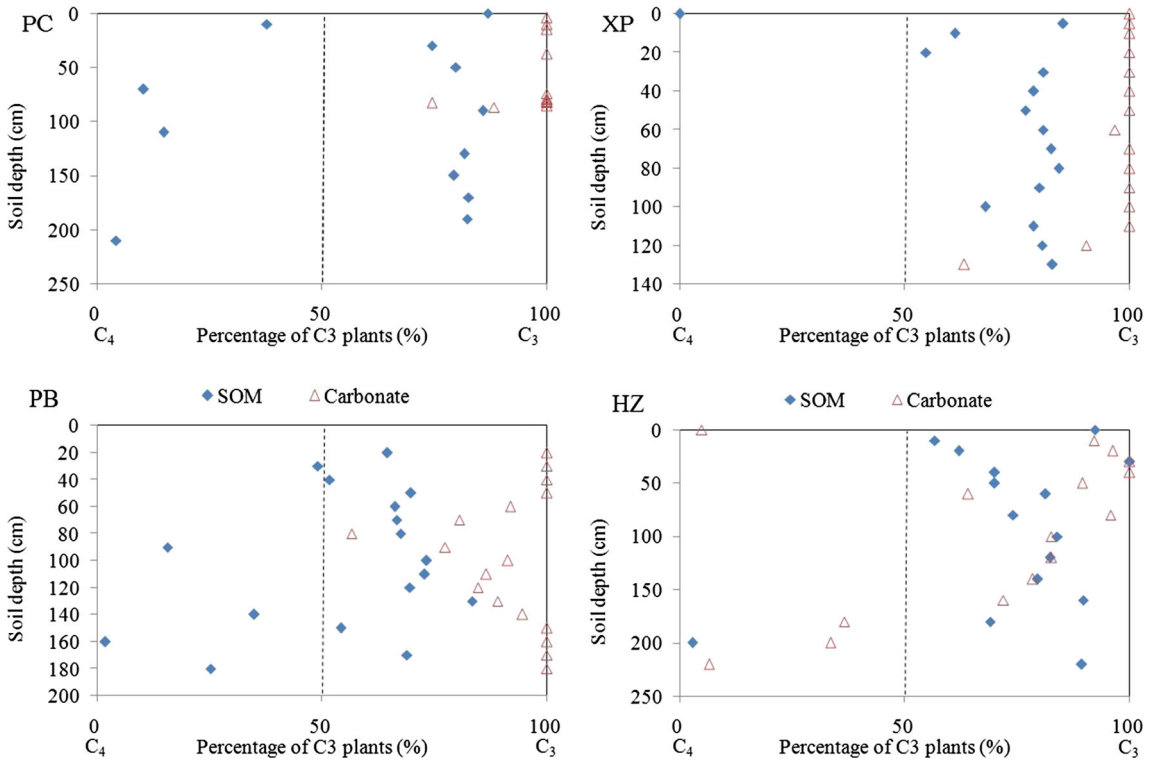

Fig. 7 Percentage of C3 plants calculated using $\delta^{13}C$ values of organic matter ($\delta^{13}C_{SOM}$) and disseminated carbonate ($\delta^{13}C_{SC}$)

$\delta^{13}C_{SC}$ at HZ demonstrated more C_4 plants than that calculated by $\delta^{13}C_{SOM}$ especially at the deeper depths (Fig. 7). The value at 0 cm was calculated using a notably high $\delta^{13}C_{SC}$ (1.31 ‰), which may have been caused by the mix of detritus based on the geomorphic features, with weathered rocks exposed in the soil, and at the sampling site, weathered rocks is on the soil site (Fig. 2).

The vertical distribution of $\delta^{13}C_{SC}$ and $\delta^{13}C_{SOM}$ was compared and is shown in Fig. 6. It can be seen that the $\delta^{13}C_{SC}$ shows a smaller and more continuous variation trend than the $\delta^{13}C_{SOM}$. The potential reason that contributes to their differences is overprinting, which refers to the imposition of later climatic information on previous information (Cerling 1984). The turnover rate of organic matter especially that in the top soil (about 10^{-1}–10^{-5} a^{-1}) (Table 3) is relatively higher compared with the rates of soil carbonate formation (10^{-6} to 10^{-5} mol/cm^2/year) (Cerling and Quade 1993), which means that detailed variation information of $\delta^{13}C_{SOM}$ in short time may not be recorded in the $\delta^{13}C_{SC}$, and the $\delta^{13}C_{SC}$ tends to reflect more average information of environmental change.

Carbonate content in loess is often used to indicate the climate change (Fang et al. 1996; Rao et al. 2006; Cheng et al. 2007; Peng et al. 2003). Higher carbonate content usually indicates cold and dry climate, and lower carbonate content usually indicates warm and wet climate. The $\delta^{13}C_{SC}$ shows a similar varying tendency as carbonate content at each site, suggesting a reflection of climate change by the $\delta^{13}C_{SC}$. This can be explained considering arid climate is more suitable for the growth of C_4 plant with higher $\delta^{13}C$ value, and wet climate is more suitable for the growth of C_3 plant with lower $\delta^{13}C$ value.

The stable carbon and oxygen isotopic value have a positive linear relationship (Fig. 4). The correlation coefficient R^2 between $\delta^{13}C_{SC}$ and $\delta^{18}O_{SC}$ is much higher at HZ (0.8197) compared with PC (0.4459), XP (0.5132) and PB (0.6245). The $\delta^{13}C_{SC}$ and $\delta^{18}O_{SC}$ at HZ was also the highest (Fig. 4). The difference between HZ and other three sites is obvious. Based on previous research, the $\delta^{18}O$ values of pedogenic carbonate are generally assumed to be in equilibrium with soil water, the isotopic composition of which is related to that of meteoric water (Khadkikar et al. 2000; Schmid et al. 2006). The oxygen isotope signature of rainwater is predominantly controlled by mean annual air temperature and climate. As temperature increases, $\delta^{18}O$ values increase (Monger et al. 1998). Other possible reasons include evaporation, re-equilibration caused by carbonate dissolution and re-precipitation after rainwater entering the soil (Cerling 1984). As evaporation increases, $\delta^{18}O$ values increase (Cerling 1984). The higher $\delta^{13}C_{SC}$ and $\delta^{18}O_{SC}$ at HZ therefore indicate warmer or drier climate conditions in the carbonate formation period compared with other sites. The site HZ is in the west; the other three sites are in the middle of Guizhou Province, and the

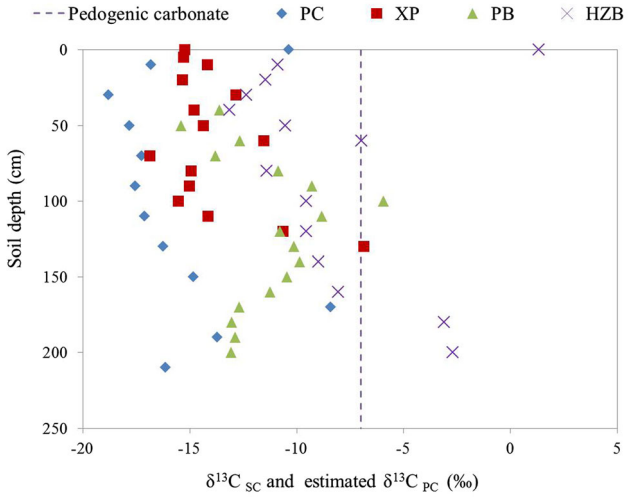

Fig. 8 $\delta^{13}C_{SC}$ and estimated $\delta^{13}C_{PC}$ values. The dots indicate the $\delta^{13}C_{SC}$ values for each site. The *lines* represent the $\delta^{13}C$ of pedogenic carbonate ($\delta^{13}C_{PC}$) estimated from average $\delta^{13}C_{SOM}$ values of the upper depth, which is about 7 ‰ for each site

site HZ is mainly affected by the southwest monsoon in history, while the sites PC, XP and PB are mainly influenced by the southeast monsoon (An et al. 1991); this difference may be a signal of the regional climate difference, which needs further study.

Conclusions

Disseminated carbonate in terra rossa is mainly composed of pedogenic carbonate, and its formation is greatly related to root activities. A large increase in $\delta^{13}C_{SOM}$ was observed at each site, which can be seen as a signal of climate change into warm and dry. This climate change happened at about 6000–8000 a BP and 12000–14000 a BP according to PC and PB, 28000 a BP according to HZ.

The $\delta^{13}C$ values of pedogenic carbonate estimated by the stable C isotope diffusion model deviate positively from the expected values, especially at sites PC, XP and PB, illustrating that C_3 plants took up a larger percentage of the vegetation when the carbonate precipitated. The percentage of C_3 plants calculated by $\delta^{13}C_{SC}$ was higher than that calculated by $\delta^{13}C_{SOM}$ at sites PC, XP and PB, further supporting that C_3 plants made up a larger percentage when carbonate precipitated. Compared with the $\delta^{13}C_{SOM}$, the $\delta^{13}C_{SC}$ tends to reflect more average variation information. Most changes in $\delta^{13}C_{SC}$ and $\delta^{13}C_{SOM}$ between adjacent sampling layers >3 ‰ are accompanied with the change in soil color and texture, suggesting a certain connection between the $\delta^{13}C$ and the soil properties. A similar varying tendency between carbonate content and $\delta^{13}C_{SC}$ was found at each site. The $\delta^{13}C_{SC}$ and $\delta^{18}O_{SC}$ values and their correlation coefficient at HZ were higher than at other sites, which may be caused by regional climate difference. In this case, the disseminated carbonate in terra rossa can provide a meaningful signal of environmental change.

Acknowledgments This work was jointly supported by the National Natural Science Foundation of China (NSFC) Grants (Nos. 41473122 and 41073096), National Key Basic Research Program of China (2013CB956702) and the Hundred Talents Program of the Chinese Academy of Sciences. We thank Geng L. for isotope analysis, Zhu X.F. and Liang X.T. for SOC content analysis. Furthermore, we are indebted to Academician & Prof. Liu C.Q. for discussion and suggestions on this study. We wish to express our sincere gratitude to anonymous reviewer for providing thorough and valuable reviews.

References

Achyuthan H, Quade J, Roe L, Placzek C (2007) Stable isotopic composition of pedogenic carbonates from the eastern margin of the Thar Desert, Rajasthan, India. Quat Int 162–163:50–60

Altay I (1997) Red Mediterranean soils in some karstic regions of Taurus mountains, Turkey. Catena 28(3):247–260

An ZS, Wu XH, Wang PX et al (1991) Changes in the monsoon and associated environmental changes in China since the last interglacial. In: Liu TS (ed) Loess, environment and global change. Science in China Press, Beijing, pp 1–29

Becze-Deak J, Langohr R, Verrecchia EP (1997) Small scale secondary $CaCO_3$ accumulations in selected sections of the European loess belt. Morphological forms and potential for paleoenvironmental reconstruction. Geoderma 76:221–252

Boutton JW (1983) Comparison of quartz and pyrex tubes for combustion of organic samples for stable carbon isotope analysis. Anal Chem 55:1832–1833

Boutton TW, Archer SR, Midwood AJ, Zitzer SF, Bol R (1998) $\delta^{13}C$ values of soil organic carbon and their use in documenting vegetation change in a subtropical savanna ecosystem. Geoderma 82:5–41

Bronger A, Bruhn RN (1997) Paleopedology of Terrae rossae—Rhodoxeralfs from quaternary calcarenites in NW Morocco. Catena 28:279–295

Buchmann N, Kao WY, Ehleringer J (1997) Influence of stand structure on carbon-13 of vegetation, soils, and canopy air within deciduous and evergreen forests in Utah, United States. Oecologia 110:109–119

Cailleau G et al (2005) Biologically induced accumulations of $CaCO_3$ in orthox soils of Biga, Ivory Coast. Catena 59(1):1–17

Candy I (2009) Terrestrial and freshwater carbonates in Hoxnian interglacial deposits, UK: micromorphology, stable isotopic composition and palaeoenvironmental significance. Proc Geol Assoc 120:49–57

Candy I, Adamson K, Gallant CE, Whitfield E, Pope R (2012) Oxygen and carbon isotopic composition of quaternary meteoric carbonates from Western and Southern Europe: their role in palaoenvironmental reconstruction. Palaeogeogr Palaeoclimatol Palaeoecol 1(11):326–328

Cerling TE (1984) The stable isotopic composition of modern soil carbonate and its relationship to climate. Earth Planet Sci Lett 71(2):229–240

Cerling TE, Quade J (1993) Stable carbon and oxygen isotopes in soil carbonates. Geophys Monogr 78:217–231

Chen QQ, Shen CD, Sun YM, Peng SL (2005) Mechanism of distribution of soil organic matter with depth due to evolution of

soil profiles at the Dinghushan Natural Reserve. Acta Pedol Sin 42(1):1–8

Cheng Z, Ma HZ, Cao GC et al (2007) The discussion about the relationship between carbonate in loess and climate environment. Yunnan Geogr Environ Res 19(3):7–14 **(in Chinese)**

Cherkinsky AE, Brovkin VA (1993) Dynamics of radiocarbon in soils. Radiocarbon 35(3):363–367

Connin S, Virginia R, Chamberlain CP (1997) Isotopic study of environmental change from disseminated carbonate in polygenetic soils. Soil Sci Soc Am J 6(61):1710–1722

Durn G (2003) Terra rossa in the Mediterranean region: parent materials, composition and origin. Geol Croat 56(1):83–100

Durn G, Ottner F, Slovenec D (1999) Mineralogical and geochemical indicators of the polygenetic nature of terra rossa in Istria, Croatia. Geoderma 91:125–150

Ehleringer JR, Buchmann N, Flanagan LB (2000) Carbon isotope ratios in belowground carbon cycle processes. Ecol Appl 10(2):412–422

Fang XM, Dai XR, Li JJ, Cao JX et al (1996) Abruptness and instability of Asian monsoon—an example from soil genesis during the last interglacial. Sci China Ser D Earth Sci 26:154–160 **(in Chinese)**

Farquhar GD, Ehleringer JR, Hubick KY (1989) Carbon isotope discrimination and photosynthesis. Annu Rev Plant Physiol Plant Mol Biol 40:503–537

Feng JL, Cui ZJ, Zhu LP (2009a) Origin of terra rossa over dolomite on the Yunnan-Guizhou Plateau, China. Geochem J 43:151–166

Feng JL, Zhu LP, Cui ZJ (2009b) Quartz features constrain the origin of terra rossa over dolomite on the Yunnan-Guizhou Plateau, China. J Asian Earth Sci 36:156–167

Feng JL, Gao SP, Zhang JF (2011) Lanthanide tetrad effect in ferromanganese concretions and terra rossa overlying dolomite during weathering. Chem der Erde Geochem 71(4):349–362

Irmak S, Aydemir S (2008) Morphology of three terra rossa soils in East Mediterranean Region, Turkey. Asian J Chem 20(4):2580–2586

ISO (2005) ISO 10390:2005 Soil quality—determination of pH. International Organization for Standardization, Geneva, Switzerland

Ji HB, Wang SJ, Ouyang ZY, Zhang S, Sun CX, Liu XM, Zhou DQ (2004a) Geochemistry of red residua underlying dolomites in karst terrains of Yunnan-Guizhou Plateau I. The formation of the Pingba profile. Chem Geol 203:1–27

Ji HB, Wang SJ, Ouyang ZY, Zhang S, Sun CX, Liu XM, Zhou DQ (2004b) Geochemistry of red residua underlying dolomites in karst terrains of Yunnan-Guizhou Plateau II. The mobility of rare earth elements during weathering. Chem Geol 203:29–50

Kelly EF, Amundson RG, Marino BD, DeNiro MJ (1991) Stable carbon isotopic composition of carbonate in Holocene grassland soils. Soil Sci Soc Am J 55:1651–1658

Khadkikar AS, Chamyal LS, Ramesh R (2000) The character and genesis of calcrete in Late Quaternary alluvial deposits, Gujarat, western India, and its bearing on the interpretation of ancient climates. Palaeogeogr Palaeoclimatol Palaeoecol 162:239–261

Kovda I, Mora CI, Wilding LP (2006) Stable isotope compositions of pedogenic carbonates and soil organic matter in a temperate climate Vertisol with gilgai, Southern Russia. Geoderma 136:423–435

Kraimer RA, Monger HC (2009) Carbon isotopic subsets of soil carbonate—a particle size comparison of limestone and igneous parent materials. Geoderma 150:1–9

Kuo TS, Liu ZQ, Li HC, Wan NJ, Shen CC, Ku TL (2011) Climate and environmental changes during the past millennium in central western Guizhou, China as recorded by Stalagmite ZJD-21. J Asian Earth Sci 40:1111–1120

Landi A, Anderson DW, Mermut AR (2003) Organic carbon storage and stable isotope composition of soils along a grassland to forest environmental gradient in Saskatchewan. Can J Soil Sci 83(4):405–414

Li DJ, Ji HB (2015) Determining CO_2 consumption from elemental change in soil profiles developed on carbonate and silicate rocks. Chin J Geochem 34(2):177–193

Li XJ, Ogrinc N, Hamilton SK, Szramek K, Kanduc T, Walter LM (2009) Inorganic carbon isotope systematics in soil profiles undergoing silicate and carbonate weathering (Southern Michigan, USA). Chem Geol 264:139–153

Liu WJ, Liu CQ, Zhao ZQ, Xu XF, Liang CS, Li LB, Feng JY (2013) Elemental and strontium isotopic geochemistry of the soil profiles developed on limestone and sandstone in karstic terrain on Yunnan-Guizhou Plateau, China: implications for chemical weathering and parent materials. J Asian Earth Sci 67–68:138–152

McCrea JM (1950) On the isotopic chemistry of carbonates and paleotemperature scale. J Phys Chem 18:849–857

Metting F, Smith J, Amthor J (1999) Science needs and new technology for soil carbon sequestration. In: Rosenberg N, Izaurralde R, Malone E (eds) Carbon sequestration in soils-science, monitoring, and beyond. Proceedings of the St. Michaels Workshop. Battelle Press, Columbus, pp 1–34

Miller DL, Mora CI, Driese SG (2007) Isotopic variability in large carbonate nodules in Vertisols: implications for climate and ecosystem assessments. Geoderma 142:104–111

Monger HC, Cole DR, Gish JW, Giordano TH (1998) Stable carbon and oxygen isotopes in Quaternary soil carbonates as indicators of ecogeomorphic changes in the northern Chihuahuan Desert, USA. Geoderma 82:137–172

Nordt LC, Hallmark CT, Wilding LP, Boutton TW (1998) Quantifying pedogenic carbonate accumulations using stable carbon isotopes. Geoderma 82:115–136

Pankaj S (2001) Paleoclimatic implications of pedogenic carbonates in Holocene soils of the Gangetic Plains, India. Palaeogeogr Palaeoclimatol Palaeoecol 172:207–222

Peng HX, Li CA, Yang GF et al (2003) Carbonate content variation of loess and paleo-climate record: taking Hongzuisi section in Lanzhou as an example. Geol Sci Technol Inf 22(1):53–55 **(in Chinese)**

Quade J, Cerling TE, Bowman JR (1989) Systematic variations in the carbon and oxygen isotope composition of pedogenic carbonate along elevation transects in the Southern Great Basin, U.S.A. Geol Soc Am Bull 101:464–475

Quade J, Rech JA, Latorre C, Betancourt JL, Gleeson E, Kalin M (2007) Soils at the hyperarid margin: the isotopic composition of soil carbonate from the Atacama Desert, Northern Chile. Geochim Cosmochim Acta 71:3772–3795

Rao ZG, Chen FH, Wang HB, Zhang JW, Zhu ZY (2006) Eastern Asian summer monsoon variation during MIS 5e as recorded by paleosol S1 at Jiuzhoutai loess section. Mar Geol Quat Geol 26:103–111 **(in Chinese)**

Rao ZG, Xu YB, Xia DS, Xie LH, Chen FH (2013) Variation and paleoclimatic significance of organic carbon isotopes of Ili loess in arid Central Asia. Org Geochem 63:56–63

Royer DL (1999) Depth to pedogenic carbonate horizon as a paleoprecipitation indicator? Geology 27:1123–1126

Schmid S, Worden RH, Fisher QJ (2006) Variations of stable isotopes with depth in regolith calcite cements in the Broken Hill region, Australia: palaeoclimate evolution signal? J Geochem Explor 89:355–358

Stevenson BA, Kelly EF, McDonald EV, Busacca AJ (2005) The stable carbon isotope composition of soil organic carbon and pedogenic carbonates along a bioclimatic gradient in the Palouseregion, Washington State, USA. Geoderma 124:37–47

Stuiver M, Polach H (1977) Reporting of ^{14}C data. Radiocarbon 19:355–363

Trumbore SE (1997) Potential responses of soil organic carbon to global environmental change. Proc Natl Acad Sci 94(16):8284–8291

Valter B, Alessandra P, Pietro M, Elisabetta B, Enza A (1992) Influence of climate on the iron oxide mineralogy of terra rossa. Clays Clay Miner 40(1):8–13

Verrecchia EP (2011) Pedogenic carbonates. In: Reitner J, Thiel V (eds) Encyclopedia of Geobiology. Encyclopedia of earth sciences series, Springer, pp 721–725. doi:10.1007/978-1-4020-9212-1

Wallace G, Sparks R, Lowe D, Pohl K et al (1987) The New Zealand accelerator mass spectrometry facility. Nucl Instrum Methods Phys Res Sect B: Beam Interact Mater Atoms 29(1–2):124–128

Wei X, Ji HB, Li DJ, Zhang FL, Wang SJ (2013) Material source analysis and element geochemical research about two types of representative bauxite deposits and terra rossa in western Guangxi, southern China. J Geochem Explor 133:68–87

Wynn JG, Harden JW, Fries TL (2006) Stable carbon isotope depth profiles and soil organic carbon dynamics in the lower Mississippi Basin. Geoderma 131:89–109

Xing CP (1998) Studies on ^{14}C age and ^{14}C tracing for subtropical forest soils in south China. Guangzhou Institute of Geochemistry, Chinese Academy of Sciences, Guangzhou, pp 19–20 (**in Chinese**)

Zhu SF, Liu CQ (2006) Vertical patterns of stable carbon isotope in soils and particle-size fractions of karst areas, Southwest China. Environ Geol 50:1119–1127